

Article

Gem-Diol and Hemiacetal Forms in Formyl Pyridine and Vitamin-B-Related Compounds: Solid-State NMR and Single-Crystal X-Ray Diffraction Studies

Ayelén Florencia Crespi, Daniel Vega, Ana K. Chattah, Gustavo Alberto Monti, Graciela Yolanda Buldain, and Juan Manuel Lázaro-Martínez

J. Phys. Chem. A, **Just Accepted Manuscript** • DOI: 10.1021/acs.jpca.6b07898 • Publication Date (Web): 15 Sep 2016

Downloaded from <http://pubs.acs.org> on September 15, 2016

Just Accepted

“Just Accepted” manuscripts have been peer-reviewed and accepted for publication. They are posted online prior to technical editing, formatting for publication and author proofing. The American Chemical Society provides “Just Accepted” as a free service to the research community to expedite the dissemination of scientific material as soon as possible after acceptance. “Just Accepted” manuscripts appear in full in PDF format accompanied by an HTML abstract. “Just Accepted” manuscripts have been fully peer reviewed, but should not be considered the official version of record. They are accessible to all readers and citable by the Digital Object Identifier (DOI®). “Just Accepted” is an optional service offered to authors. Therefore, the “Just Accepted” Web site may not include all articles that will be published in the journal. After a manuscript is technically edited and formatted, it will be removed from the “Just Accepted” Web site and published as an ASAP article. Note that technical editing may introduce minor changes to the manuscript text and/or graphics which could affect content, and all legal disclaimers and ethical guidelines that apply to the journal pertain. ACS cannot be held responsible for errors or consequences arising from the use of information contained in these “Just Accepted” manuscripts.

1
2
3 ***Gem*-Diol and Hemiacetal Forms in Formyl Pyridine and Vitamin-B₆-Related**
4 **Compounds: Solid-State NMR and Single-Crystal X-Ray Diffraction Studies.**
5
6

7
8 Ayelén Florencia Crespi,[†] Daniel Vega,[‡] Ana Karina Chattah,[‡] Gustavo Alberto Monti,[‡]
9

10 Graciela Yolanda Buldain,^{†,‡} Juan Manuel Lázaro-Martínez.^{†, §,*}
11
12

13
14
15 [†]Universidad de Buenos Aires, Facultad de Farmacia y Bioquímica, Departamento de
16 Química Orgánica, Junín 956 (C1113AAD), CABA, Argentina.
17

18
19 [‡]Departamento de Física de la Materia Condensada, Comisión Nacional de Energía
20 Atómica, Av. Gral. Paz 1499 (1650) San Martín, Buenos Aires, Argentina and Escuela de
21 Ciencia y Tecnología, Universidad Nacional de General San Martín, Buenos Aires,
22 Argentina.
23
24

25
26 [‡]CONICET, Godoy Cruz 2290 (C1425FQB), CABA, Argentina.
27

28
29 [‡]FaMAF-Universidad Nacional de Córdoba & IFEG-CONICET, Medina Allende s/n
30 (X5000HUA), Córdoba, Argentina.
31

32
33 [§]IQUIFIB-CONICET, Junín 956 (C1113AAD), CABA, Argentina.
34
35

36
37
38
39
40
41 **Abstract.**
42

43
44 The *gem*-diol moieties of organic compounds are rarely isolated or even studied in the solid
45 state. Here, liquid- and solid-state NMR, together with single-crystal X-ray diffraction
46 studies, were used to show different strategies to favor the *gem*-diol or carbonyl moieties
47 and to isolate hemiacetal structures in formylpyridine and vitamin-B₆-related compounds.
48 The change in position of the carbonyl group in pyridine compounds had a clear and direct
49 effect on the hydration, which was enhanced by trifluoroacetic acid addition. Due to their
50
51
52
53
54
55
56
57
58

59
60

* Corresponding author. Lázaro-Martínez, J.M. (Tel./fax: +54-11-5287-4323; e-mails:
lazarojm@ffyb.uba.ar / jmlazaromartinez@gmail.com).

1
2
3 biochemical importance, vitamin-B₆-related compounds were studied with emphasis on the
4 elucidation of the *gem*-diol, cyclic hemiacetal or carbonyl structures that can be obtained in
5
6 different experimental conditions. Particularly, new racemic mixtures for the cyclic
7
8 hemiacetal structure from pyridoxal are reported in trifluoroacetate and hydrochloride
9
10 derivatives.
11
12
13
14
15
16

17 **1. Introduction.**

18
19 The synthesis of novel molecules that act as ligands for various heavy metal ions, such as
20 those containing *gem*-diol moieties in their structures, is a field that is being widely studied
21
22 to obtain new polymeric materials and / or metal complexes due to the applications in the
23
24 synthesis of paramagnetic 3d transition metal clusters.¹ A geminal diol or *gem*-diol is the
25
26 product of the addition of water to a carbonyl group of an aldehyde or ketone. Such
27
28 compounds are rarely stable and infrequently observed in the liquid or solid state since the
29
30 moisture balance is largely dependent on the structure. For example, 99.99% of
31
32 formaldehyde but only 58% of acetaldehyde in water at 20°C exist in the hydrated form.² In
33
34 turn, these structures are rare and can seldom be isolated as such, because they quickly
35
36 revert to the aldehyde or ketone that originated them. However, we have previously reported
37
38 the isolation of a *gem*-diol form for the 2-imidazolecarboxaldehyde molecule, with no
39
40 remainder of the aldehyde moiety in the solid state.³
41
42
43
44
45
46
47

48
49 Particularly, imidazole and pyridine molecules containing carbonyl groups are widely used
50
51 for the synthesis of metal complexes with relevance in medicinal and coordination
52
53 chemistry.⁴⁻⁶ Sartzi *et al.* studied the use of di(2-pyridyl)ketone [(Py)₂C=O] as an organic
54
55 ligand for the synthesis of metal complexes.⁷ Efthymiou *et al.* expanded the number and
56
57 variety of carbonyl compounds, but observed the *gem*-diol form only when the X-ray
58
59 crystallographic analysis was done in single-crystal samples corresponding to metal
60

1
2
3 complexes formed from carbonyl ligands.⁸ Tasiopoulos and Perlepes studied formylpyridine
4
5 compounds for the development of coordination complexes with transition metal ions, with
6
7 emphasis on “diolate high-spin molecules” and “single-molecule magnets”.^{1,9} Particularly,
8
9 the synthesis of new single-molecule magnets is of great interest because they are promising
10
11 candidates to be applied in spintronics and quantum computing.^{10–13}
12
13

14
15 *Gem*-diol moieties in metal complexes containing pyridine carbonyl compounds have so far
16
17 been elucidated through single-crystal X-ray diffraction studies, but the electronic effects of
18
19 the ligands have been not taken into account. In this sense, a Cu(II)-complex with 2-
20
21 formylpyridine molecules (**A₁**) presents the *gem*-diol moiety in single crystals obtained from
22
23 water solutions and CuCl₂,¹⁴ demonstrating that the presence of water affects the
24
25 functionalization of the ligand, preventing the aldehyde form in the crystal lattice of the
26
27 copper complex. In contrast, the lower reactivity of the aldehyde group in 3-formylpyridine
28
29 (**A₃**) towards the addition of water explains that in the different reported complexes with
30
31 copper¹⁵ or zinc¹⁶ ions the formyl group remains in aqueous media. Furthermore, the
32
33 aldehyde moiety has been observed for zinc complexes of 2-formylpyridine (**A₁**) when the
34
35 single crystals were obtained from dissolutions in CH₂Cl₂ or CH₂Cl₂/THF with addition of
36
37 petroleum ether (b.p. 70-90 °C) in the absence of water molecules.¹⁷ Moreover, a rhenium
38
39 complex with **A₁** in methanol renders the hemiacetal structure¹⁸ as a consequence of the
40
41 addition of methanol to the aldehyde group in **A₁**, due to the higher reactivity of the formyl
42
43 moiety at the second position of the pyridine system than at the third one in 3-
44
45 formylpyridine compound (**A₂**). However, no reports of metal complexes containing the 4-
46
47 formylpyridine molecules (**A₃**) have yet been reported. In addition, no nuclear magnetic
48
49 resonance (NMR) studies have been performed to these compounds. In particular, solid-state
50
51 NMR (*ss*-NMR) has allowed overcoming the challenges inherent in studying non-crystalline
52
53 materials that cannot be characterized by single-crystal X-ray diffraction techniques, being
54
55
56
57
58
59
60

1
2
3 an ideal technique to focus on the possibility to render the *gem*-diol forms and their stability,
4
5 obtained from the corresponding carbonyl monomers commonly used in the area.^{1,14,17-23}
6
7

8 In this context, the aim of this work was to study the *gem*-diol generation in pyridine
9
10 molecules bearing carbonyl groups. In addition, vitamin-B₆-related compounds were
11
12 analyzed due to their importance in biochemical processes,^{24,25} with emphasis on the
13
14 structural elucidation that can be observed in their reactions.²⁶⁻²⁸ Liquid-state (*ls*-NMR) and
15
16 *ss*-NMR and single-crystal X-ray diffraction techniques, were used to elucidate the *gem*-diol
17
18 or carbonyl moieties and the possibility to isolate hemiacetal structures in some cases.
19
20
21
22
23

24 25 **2. Experimental Section.**

26 27 **2.1 Synthesis.**

28
29 Trifluoroacetic acid (TFA, 99%), 2-formylpyridine (**A**₁, 99%), 3-formylpyridine (**A**₂, 98%),
30
31 4-formylpyridine (**A**₃, 97%), 3-chloro-4-formylpyridine (**A**₄, 97%), 2-chloro-3-
32
33 formylpyridine (**A**₅, 97%), di(2-pyridyl)ketone (**K**₆, 99%), pyridoxal hydrochloride (**A**₇.HCl,
34
35 ≥99%), pyridoxal-5'-phosphate (**A**₈, ≥98%), deuterium oxide (D₂O, 99.9 atom %D) and
36
37 dimethylsulfoxide-*d*₆ (DMSO-*d*₆, 99.96 atom %D) were purchased from Sigma-Aldrich and
38
39 were used without further purification.
40
41
42

43
44 The general quantitative synthesis of the corresponding neutral *gem*-diol solid forms for 4-
45
46 formylpyridine (**A**₃) and 3-chloro-4-formylpyridine (**A**₄) consists in dissolving 40 mmol of
47
48 **A**₃ or **A**₄ in 3 mL of distilled water, which produces the spontaneous crystallization of the
49
50 *gem*-diol compounds (**H**₃ melting point = 70-72°C and **H**₄ melting point = 84-86°C).
51
52

53
54 The solid pyridinium-trifluoroacetate derivatives containing *gem*-diol (**H**₁.TFA and
55
56 **H**₃.TFA) or carbonyl moieties (**A**₂.TFA), were obtained by incubation of 50 mmol of **A**₁, **A**₂
57
58 and **A**₃ in 3 mL of a solution of 1% of water in TFA for 24 h at room temperature. Then, the
59
60 TFA solutions were lyophilized and the solid samples were collected and stored in a

1
2
3 desiccator prior to the NMR measurements. Particularly, when the trifluoroacetate
4 derivatives from **A_{2,3}** (50 mmol) were placed in 5 mL of ethanol 95% for 72 h at room
5 temperature and then dried under vacuum, they were completely oxidized to the
6 corresponding carboxylic acid compounds (**CA_{2,3}.TFA**).

7
8
9
10
11
12 The solid hydrochloride pyridoxal (**A₇.HCl**) was obtained by incubation of pyridoxal (50
13 mmol) in 20 mL of HCl 5% for 72 h at room temperature, respectively. Then, the sample
14 was lyophilized and the solid sample was collected and stored in a desiccator prior to the
15 NMR measurements. The solid trifluoroacetate derivative **A₇.TFA** was obtained by
16 incubation of **A₇.HCl** (50 mmol) in 10 mL of TFA 30% for 72 h at room temperature. Then,
17 the sample was treated as in **A₇.HCl**.

29 **2.2 NMR Experiments.**

30
31 High-resolution ¹³C solid-state spectra for the different compounds were recorded using the
32 ramp ¹H-¹³C CP-MAS sequence (cross-polarization and magic angle spinning) with proton
33 decoupling during acquisition. All the *ss*-NMR experiments were performed at room
34 temperature in a Bruker Avance-II 300 spectrometer equipped with a 4-mm MAS probe.
35 The operating frequency for protons and carbons was 300.13 and 75.46 MHz, respectively.
36 Glycine was used as an external reference for the ¹³C spectra and to set the Hartmann-Hahn
37 matching condition in the cross-polarization experiments in ¹³C spectra. The recycling time
38 was set at 4 s, to obtain a compromise between the signal-to-noise ratio in a single scan and
39 the total time of the experiments performed with a number of scans between 2000 and 4000.
40 The contact time during CP was 1500 μs for ¹³C spectra for all the samples. The SPINAL64
41 sequence (small phase incremental alternation with 64 steps) was used for heteronuclear
42 decoupling during acquisition with a proton field H_{IH} satisfying $\omega_{IH}/2\pi = \gamma_H H_{IH} = 62 \text{ kHz}$.²⁹
43
44
45
46
47
48
49
50
51
52
53
54
55
56
57
58
59
60 The spinning rate for all the samples was 10 kHz.

1
2
3 The *ls*-NMR experiments were performed at room temperature in a Bruker Avance-II 300,
4 500 or Ascend-600 spectrometer. To determine the hydration of the carbonyl group, ~30 mg
5
6 of each compound was dissolved in a D₂O or D₂O solution containing 1% of TFA.
7
8
9

10 11 12 13 **2.3 Single-crystal X-ray studies.**

14
15 Single-crystal samples were isolated from the slow evaporation of each solution at room
16
17 temperature where the compound of interest was dissolved or obtained as mentioned above.
18
19 Single-crystal X-Ray diffraction data were collected at room temperature, using a Gemini A
20
21 diffractometer, Oxford Diffraction, Eos CCD detector with graphite-monochromated MoK α
22
23 ($\lambda=0.71073$ Å) radiation. Data-collection strategy and data reduction followed standard
24
25 procedures implemented in the CrystAlisPro software. Different independent reflections
26
27 were collected for each sample and they are specified in the Supporting Information. The
28
29 structures were solved using SHELXS-97 program³⁰ and refined using the full-matrix LS
30
31 procedure with SHELXL-2014/7.³¹ Anisotropic displacement parameters were employed for
32
33 non-hydrogen atoms. All hydrogen atoms were located at the expected positions and they
34
35 were refined using a riding model.
36
37
38
39
40
41
42

43 44 **3. Results & Discussion.**

45 46 **3.1 Studies in formylpyridines.**

47
48 In order to study the reactivity of water addition in formylpyridine isomers, each compound
49
50 was dissolved in D₂O and studied by *ls*-NMR experiments (Table 1). The ¹H-NMR spectra
51
52 for all the isomers showed the presence of the *gem*-diol moieties in D₂O at a proton chemical
53
54 shift around (-CH(OH)₂) depending on the position in the pyridine ring (Figure 1 and
55
56 Supporting Information). Based on the integration of each ¹H-NMR signal for the *gem*-diol
57
58 ($\delta^1\text{H} = 5.70\text{-}6.30$ ppm) and/or the aldehyde ($\delta^1\text{H} = 9.19\text{-}10.40$ ppm), it was possible to
59
60

obtain the relative content in terms of each functional moiety (Table 1). From these results, we concluded that the most reactive compound for the addition of water was 4-formylpyridine (**A**₃) (54%) followed by 2-formylpyridine (**A**₁) (44%) and 3-formylpyridine (**A**₂) (11%). This fact is justified given the π -deficient character of the pyridine ring where the most electron-deficient positions are 2, 4 and 6 in comparison with 3 and 5, explaining that 3-formylpyridine had the lowest hydrate percent. Moreover, the complete hydration in 2- and 4-formylpyridines can be obtained with 1% of TFA in D₂O according with the ¹H-NMR spectrum (Figure 1). However, **A**₂ was not completely hydrated even with a higher TFA concentration (Table 1) since the third position of the pyridine system was not equally affected by the inductive effect of the system in comparison with the other positions.

Since all the formylpyridine isomers are liquid at room temperature, we prepared the solid trifluoroacetate derivatives to be studied by *ss*-NMR, and, in the cases where the substance rendered single crystals, they were studied through X-ray diffraction. Figure 2 shows the ¹³C CP-MAS spectra for the products obtained for the corresponding trifluoroacetate derivatives or neutral form of the formylpyridines and other related solid compounds commercially available.

Table 1. Amount of *gem*-diol and aldehyde forms for the indicated carbonyl compounds determined by ¹H-NMR.

Compound	¹ H-NMR experiment			
	D ₂ O		D ₂ O-TFA	
	<i>gem</i> -diol	aldehyde	<i>gem</i> -diol	aldehyde
2-CHO-Pyridine (A ₁)	40	60	100	-
3-CHO-Pyridine (A ₂)	10	90	85	15
4-CHO-Pyridine (A ₃)	50	50	100	-

3-Cl-4-CHO-Pyridine (A₄)	83 (47) ^a	17 (53) ^a	100	-
2-Cl-3-CHO-Pyridine (A₅) ^b	41 (-) ^a	59 (100) ^a	60	40
di(2-pyridyl)ketone (K₆)	3	97 ^c	100	-
Pyridoxal.HCl (A₇.HCl)	100 ^d	-	100 ^d	-
Pyridoxal-5'-phosphate (A₈) ^e	73.8 (94) ^a	26.2 (6) ^a	75.2 ^b	24.8 ^b

^aIn DMSO-*d*₆.

^bThe reported values are related to the relative content of the *gem*-diol and aldehyde forms since other compounds are also present in the mixture (see the text and Supporting Information for additional details).

^cThe reported value is for the ketone form.

^dThe reported values refer to the cyclic hemiacetal in D₂O, D₂O-TFA and DMSO-*d*₆. However, the *gem*-diol moiety was quantitatively obtained when the solid **A₇.HCl** was treated with D₂O/NaOH solution.

^eThe aldehyde form was quantitatively obtained when the solid **A₈** was treated with D₂O/NaOH.

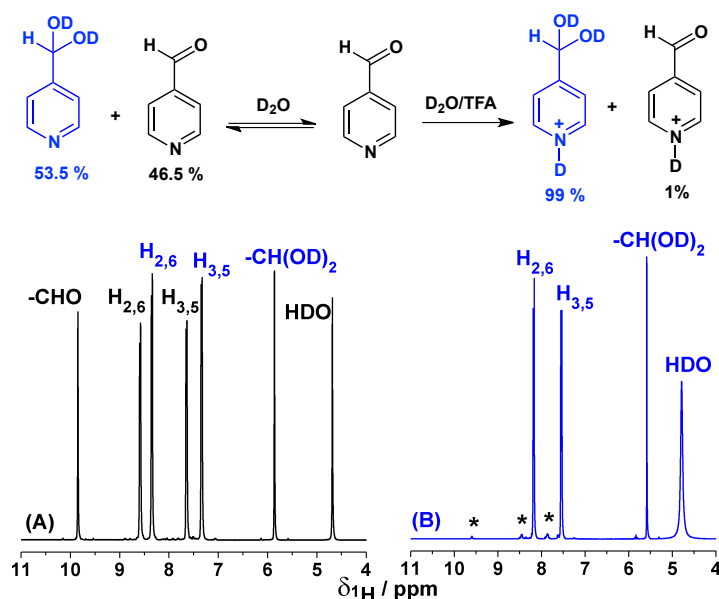


Figure 1. ¹H-NMR spectra for 4-formylpyridine (**A₃**) in the presence of D₂O (A) and D₂O-TFA (B). The asterisk in spectrum B indicates the residual signal of the carbonyl form.

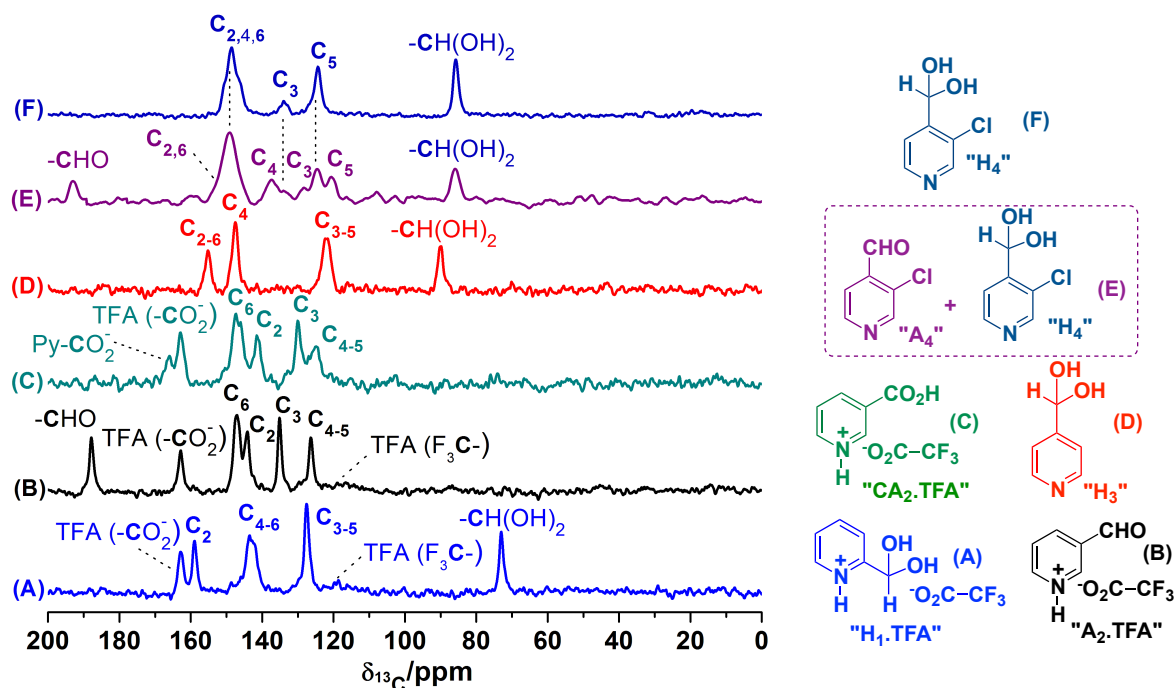


Figure 2. ^{13}C CP-MAS spectra for the solids obtained after the treatment of the following compounds in different experimental conditions: 2-formylpyridine (A_1) in TFA (H_1TFA , A), 3-formylpyridine (A_2) in TFA (A_2TFA , B) and the A_2TFA treated with ethanol (CA_2TFA , C). Solid obtained with 4-formylpyridine (A_3) in water (H_3 , D). A solid commercial sample of 3-chloro-4-formylpyridine (A_4) ($\text{A}_4 + \text{H}_4$, E) and the solid obtained after the treatment of A_4 with water (H_8 , F).

Even when all the pyridine derivatives were incubated in TFA under the same experimental conditions, depending on the position of the formyl group, it was possible to isolate solids where the aldehyde or *gem*-diol content was different. The ^{13}C CP-MAS spectra (Figure 2A and Figure 2B) showed that, in TFA, A_1 presented the *gem*-diol moieties ($\delta^{13}\text{C} = 73.3$ ppm, $-\text{CH}(\text{OH})_2$, Figure 2A), whereas A_2 crystallized as the corresponding aldehyde (A_2TFA) ($\delta^{13}\text{C} = 188.2$ ppm, $-\text{CHO}$, Figure 2B). In contrast, when A_2TFA was incubated in ethanol, single crystals of 3-carboxypyridine (CA_2TFA) were obtained ($\delta^{13}\text{C} = 166.3$ ppm, $-\text{CO}_2\text{H}$, Figure 2C). However, this crystallographic structure has been previously reported.³² The ^{13}C

1
2
3 CP-MAS spectrum for **CA₂.TFA** showed that the oxidation of the formyl group in **A₂** was
4 completed in this condition since no signals of the aldehyde form (**A₂**) were observed in the
5
6
7
8
9
10
11
12
13
14
15
16
17
18
19
20
21
22
23
24
25
26
27
28
29
30
31
32
33
34
35
36
37
38
39
40
41
42
43
44
45
46
47
48
49
50
51
52
53
54
55
56
57
58
59
60
CP-MAS spectrum for **CA₂.TFA** showed that the oxidation of the formyl group in **A₂** was completed in this condition since no signals of the aldehyde form (**A₂**) were observed in the *ls*- or *ss*-NMR spectra (Figure 2C). These results indicate that the solid-state NMR through ¹³C CP-MAS spectra is the best screening for the identification of the *gem*-diol groups in a solid sample by observing the range of 70-100 ppm of ¹³C chemical shift. This must be done prior to the dissolution in deuterated solvents where the proportion of carbonyl and *gem*-diol moieties change depending on the properties of the medium, not being representative of the real content in the solid state. In addition, a salt was formed between the pyridine compounds and TFA, which was evidenced from the signal of the carboxylate group at 160.5 ppm (CF₃CO₂⁻) and the carbon corresponding to the trifluoromethyl group (CF₃CO₂⁻) at ~120 ppm in the ¹³C CP-MAS spectra.³³

Interestingly, in a particular ratio of 4-formylpyridine:water (4 mL:3 mL), it was possible to obtain single crystals suitable for X-ray studies and to find the corresponding *gem*-diol form in the solid state. However, González-Mantero *et al.* have previously reported the corresponding structure as a by-product of a particular chemical reaction where the *gem*-diol form was not the objective of the work.³⁴ Also, Majerz *et al.* studied a ionic adduct between **A₃** and 2,6-dichloro-4-nitrophenol.³⁵ In the same way, 4-formylpyridine (**A₃**) rendered quantitative solid sample under the *gem*-diol form (**H₃**) from the treatment of **A₃** with water (5 mL:3 mL), although the 4-carboxypyridine (**CA₃**) was elucidated by X-ray results obtained from the incubation of the trifluoroacetate sample of **H₃** in ethanol (Figure 3). On the other hand, the solid aldehyde 3-chloro-4-formylpyridine (**A₄**) commercially available is in a mixture of aldehyde:*gem*-diol of 0.53:0.47 according with the ¹H-NMR spectrum in DMSO-*d*₆. When the solid **A₄** was treated with water, the *gem*-diol crystallized as the only product according with the *ss*-NMR spectrum (Figure 2F and Table 1). Moreover, single

crystals for **H₄** were analyzed by X-ray diffraction, showing the *gem*-diol moieties in the crystal lattice (Figure 3 and Figure S27 and Figure S28).

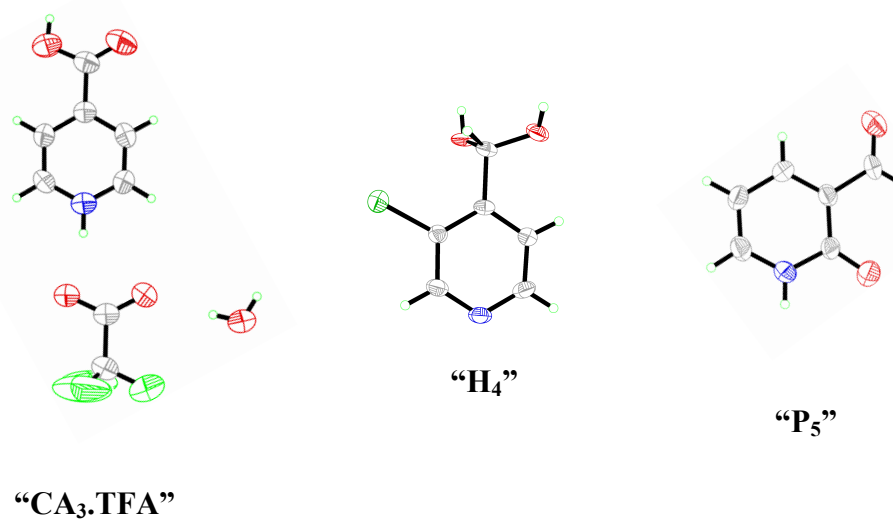


Figure 3. Crystal structures for 4-carboxypyridinium trifluoroacetate (**CA₃.TFA**), *gem*-diol form of 3-chloro-3-formylpyridine (**H₄**), and 3-formyl-2-pyridone (**P₅**). The displacement ellipsoids for the non-H atoms in the figure were drawn at the 50% probability level.

For the 2-chloro-3-formylpyridine (**A₅**), only the aldehyde form (92.6%) was present and a minority content of the 3-formyl-2-pyridone (**P₅**, 7.4%) was observed in the ¹H-NMR spectrum in DMSO-*d*₆ (Figure S13). When these solid chloro-formylpyridines (**A₄₋₅**) were dissolved in D₂O, the *gem*-diol content increased in each sample in comparison with the results in DMSO-*d*₆ according to NMR results. This is indicative of the higher reactivity of the nucleophilic addition of water to the aldehyde group than the corresponding derivatives without chlorine in their structure (Table 1). Interestingly, the ¹H-NMR spectrum of 2-chloro-3-formyl-pyridine (**A₅**) in D₂O showed that the contents of aldehyde and *gem*-diol forms were 21.3 and 14.7%, respectively. The remaining 64% was associated with a 3-formyl-2-pyridone (**P₅**) as a consequence of the nucleophilic substitution of chlorine by water molecules (Figure S11). It is important to point out that the incubation of **A₅** in water

1
2
3 rendered single crystals, where the 2-pyridone structures were elucidated by X-ray
4 diffraction studies (Figure 3, Figure S29 and Figure S30). These results indicate that the fact
5 that 3-formyl-2-pyridone (**P**₅) was obtained in 64% in water was due to the higher reactivity
6 for the nucleophilic aromatic substitution than the addition of water to the carbonyl group at
7 the third position of the aromatic system in **A**₅. Thus, the *gem*-diol form (**H**₅) was obtained in
8 14.7% with 21.3% of the aldehyde (**A**₅) (Table 1). The same analysis in D₂O-TFA showed
9 that the amounts of aldehyde, *gem*-diol and 2-pyridone forms for **A**₅ were 38.6%, 57.9% and
10 3.5%, respectively, indicative that the acidic medium increases the addition of water to the
11 aldehyde group against the substitution of the chloride at the second position (Table 1).
12
13

14
15 Finally, a di(2-pyridyl)ketone (**K**₆) was studied in the liquid-state in D₂O, where only 3%
16 was hydrated, giving rise to the *gem*-diol moiety in the ¹H-NMR spectrum (Table 1). Also,
17 the treatment of **K**₆ with water rendered a solid where, according with the ¹³C CP-MAS
18 spectrum (Figure 4A), only the ketone form was present. Even when the ketone carbon is
19 next to the second position of both electron-withdrawing pyridine rings, the effect on the
20 nucleophilic addition of water cannot be observed in D₂O solution since only 3%
21 corresponded to the *gem*-diol form, and it was necessary to add TFA to force the reaction
22 (Table 1). A possible explanation may be the hydrophobic:hydrophilic balance of the
23 molecule, which disfavors the nucleophilic attack of water. Then, the addition of TFA to an
24 aqueous solution containing **K**₆ produced the *gem*-diol form in an excellent yield as well as
25 single crystals, demonstrating again the *gem*-diol moiety and the disposition of the aromatic
26 rings in the crystal lattice (Figure 4). The ¹³C CP-MAS spectrum for the TFA crystals
27 obtained from **K**₆ (**H**₆.TFA + **K**₆.TFA) shows that most of the compound is present as *gem*-
28 diol form with traces of the ketone moieties, having into account the ¹³C resonance signal at
29 183.3 ppm, which presents a shift to low frequency values after the protonation of the
30 pyridine system in comparison with the non-protonated di(2-pyridyl)ketone ($\delta^{13}\text{C}$: 196.4
31
32
33
34
35
36
37
38
39
40
41
42
43
44
45
46
47
48
49
50
51
52
53
54
55
56
57
58
59
60

ppm, $>C=O$, Figure 4). The TFA crystals of K_6 ($H_6.TFA + K_6.TFA$) dissolved in D_2O showed a similar amount of both *gem*-diol and ketone forms. However, the NMR spectrum in $DMSO-d_6$ shows only the ketone form (Figure S24), being not representative of the solid composition according with the *ss*-NMR. The X-ray results demonstrated the *gem*-diol structure for K_6 ($H_6.TFA$, Figure 4). The hydrated structure was first reported for a hydrochloride form of H_6 with structural differences in the crystal lattice since both nitrogens of the pyridine rings were in opposite direction.³⁶ In contrast, in the TFA salt reported here, both nitrogens are in the same side and the *gem*-diol is linked by hydrogen bonds with the carboxyl group of TFA (Fig. 4 and Supporting Information). Regarding reported metal complexes, the *gem*-diol forms were observed in Cu(II) or Ni(II) centers synthesized from K_6 where the *gem*-diol structure is stabilized by coordination with less importance of the metal ion and the anion used in their preparation.^{37,38} The hydration of the carbonyl group is enhanced by the slight acidification of the medium since in aqueous solution only 3% of the *gem*-diol is present, in agreement with our results reported here (Table 1).

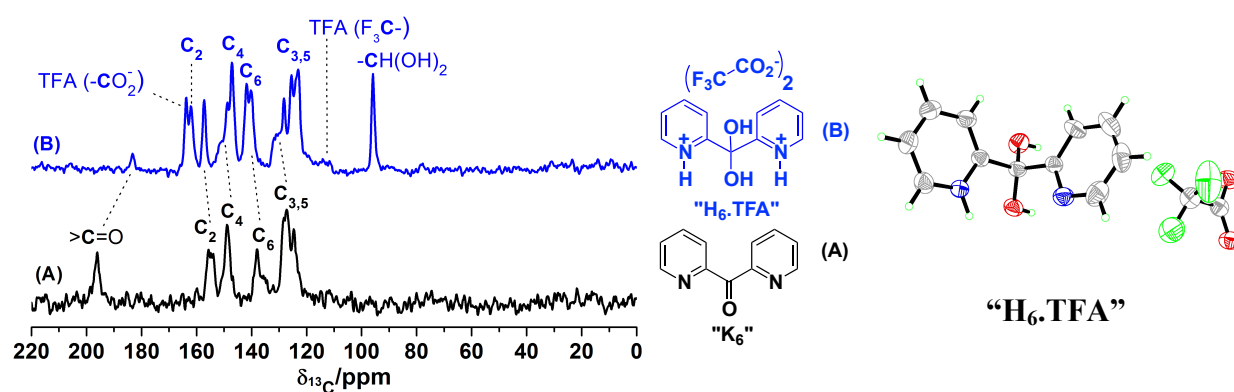


Figure 4. ^{13}C CP-MAS spectra for the commercial solid of the di(2-pyridyl)ketone (K_6) (A) and K_6 treated with TFA ($H_6.TFA + K_6.TFA$) (B). Crystal structure for $H_6.TFA$. The displacement ellipsoids for the non-H atoms in the figure were drawn at the 50% probability level.

3.2 Vitamin-B₆-related compounds:

Pyridoxal (A₇) and pyridoxal-5'-phosphate (A₈) compounds were studied having into account their biochemical importance due to their role as coenzymes in different enzymatic reactions (Figure 5). The ¹³C CP-MAS spectrum for a hydrochloride pyridoxal (A₇.HCl) sample was performed and the results are shown in Figure 5A. The *ss*-NMR spectrum indicated the absence of the aldehyde around 180-200 ppm and the presence of the corresponding *gem*-diol or hemiacetal moieties at 98.7 ppm. However, the *ls*-NMR clearly showed that the cyclic hemiacetal form (HA₇.HCl) was present for this molecule due to the magnetic inequivalence of the protons of the methylene group.³⁹ The two doublets present at 5.32 and 5.14 ppm with a *J*_{gem} coupling of 13.8 Hz in the ¹H-NMR spectrum demonstrate the cyclization involving the hydroxymethylene and the carbonyl group (Figure 5 and Figure S14).

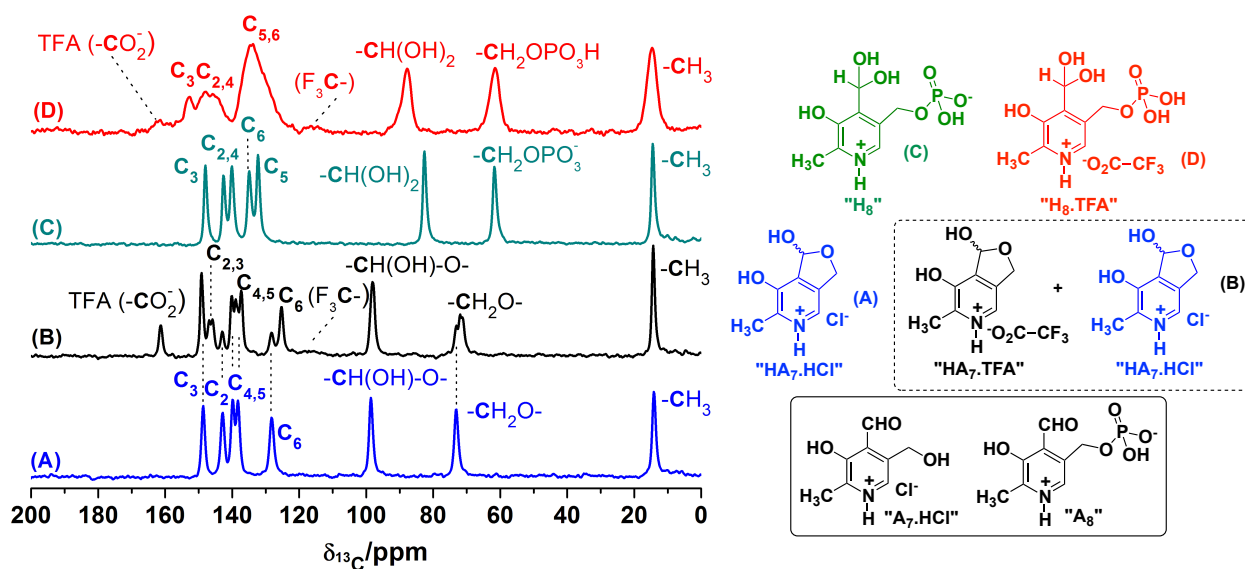
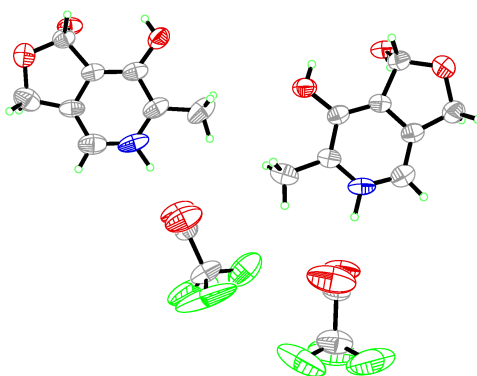


Figure 5. ¹³C CP-MAS spectra for pyridoxal.HCl (HA₇.HCl, A), pyridoxal.HCl incubated with TFA (HA₇.HCl + HA₇.TFA, B), pyridoxal-5'-phosphate (H₈, C), and pyridoxal-5'-phosphate treated with TFA (H₈.TFA, D).

1
2
3 The single-crystal X-ray diffraction structure resolved for the TFA salts allowed us to
4 confirm the cyclic hemiacetal formation together with the racemic structure that can also be
5
6 confirmed (Figure 6), something that is not possible from the NMR spectra in Figure 5.
7
8
9
10 Manohar *et al.* reported the X-ray structure for the pyridoxal molecule in the neutral form,
11 where the hemiacetal and the zwitterionic forms were present, but the racemic mixture was
12 not obtained.⁴⁰ Our results show that the racemization takes place due to the intramolecular
13 cyclization and is equally probable for both sides of the planar formyl group, rendering a
14 racemic sample that was evidenced with the X-ray results (Figure 6). Since the racemization
15 cannot be deduced from the NMR spectra, optical rotation experiments were performed. The
16 aqueous solutions of the crystalline pyridoxal.TFA (**HA₇.TFA**) or pyridoxal.HCl (**HA₇.HCl**)
17 samples were optically inactive, meaning that there is no net rotation of the plane-polarized
18 light due to the racemic mixture in both solids.
19
20
21
22
23
24
25
26
27
28
29
30
31



32
33
34
35
36
37
38
39
40
41
42
43
44
45 **Figure 6.** Crystal structure for pyridoxal.TFA racemate (**HA₇.TFA**). The displacement
46 ellipsoids for the non-H atoms in the figure were drawn at the 50% probability level.
47
48
49

50
51
52 Furthermore, even when the single-crystal structure was studied only for the pyridoxal.TFA
53 compound, the ¹³C CP-MAS for the TFA salt provided additional information concerning
54 the composition of the crystalline powder obtained after the treatment with TFA of an
55 aqueous solution of the hydrochloride pyridoxal. Spectrum B in Figure 5 shows the presence
56 of both chloride and trifluoroacetate as contra-ion of the cationic pyridinium system from
57
58
59
60

1
2
3 the pyridoxal molecule, being possible the discrimination of both molecules due to the
4 different environments of each pyridine system depending on its anion (Figure 5). The
5 splitting of the NMR signals may indicate the presence of two molecules per unit cell in
6 Figure 5B. However, as determined by X-ray fluorescence, the **HA₇.TFA** sample still
7 contains a chlorine content of $3.30\pm 0.10\%$, indicative of hydrochloride content in the
8 **HA₇.TFA** solid sample. Also, some of the chemical shifts are observed for **HA₇.HCl** in the
9 **HA₇.TFA** solid sample in comparison with the pure **HA₇.HCl** sample.

10 The *ls*-NMR results for the pyridoxal hydrochloride in both D₂O and D₂O-TFA showed that
11 only the cyclic hemiacetal structure is present and stable. However, when the ¹H spectrum
12 was recorded in D₂O-NaOH, the corresponding *gem*-diol form was observed, taking into
13 account that the protons of the methylene group resonate as a singlet at 4.50 ppm, indicating
14 that the hemiacetal structure has been affected by the alkaline medium. The *gem*-diol proton
15 can be observed at 6.39 ppm (Figure S16). Although the single-crystal X-ray structure for
16 the pyridoxal hydrochloride (**A₇.HCl**) has been previously reported by Fujiwara *et al.*,⁴¹
17 where the aldehyde structure was present, our results presented here show that the cyclic
18 hemiacetal structure for **A₇.HCl** and **A₇.TFA** is the only structure present according with the
19 *ss*-, *ls*-NMR and X-ray results.

20 The last compound analyzed in this work was the pyridoxal-5'-phosphate (**A₈**), which
21 presented a well-resolved ¹³C CP-MAS spectrum (Figure 5C) for the *gem*-diol form (**H₈**),
22 since in this molecule the formation of a cyclic hemiacetal as in pyridoxal is not possible due
23 to the phosphate group at the hydroxymethylene group at the fifth position of the pyridine
24 ring. The single-crystal X-ray structure for **A₈** has been previously resolved by Fujiwara *et*
25 *al.*⁴² Nevertheless, the solid was analyzed by *ss*-NMR and the result is shown in Figure 5C.
26 The *gem*-diol form was present for the pyridoxal-5'-phosphate in the commercial sample
27 treated in water or TFA:water (1:0.01) solution. Also, a shift in the *gem*-diol carbon from
28
29
30
31
32
33
34
35
36
37
38
39
40
41
42
43
44
45
46
47
48
49
50
51
52
53
54
55
56
57
58
59
60

1
2
3 82.6 to 88.0 ppm can be observed with the formation of the TFA salt (Figure 5). The *ls*-
4 NMR results in D₂O for a commercial sample of pyridoxal-5'-phosphate showed that the
5 *gem*-diol and the aldehyde forms were present in 73.8% and 26.2%, respectively. However,
6 the ¹³C CP-MAS spectra only shows the *gem*-diol form (Figure 5). The ¹H-NMR spectrum
7 in D₂O-TFA shows a similar amount of *gem*-diol (75.2%), but a lower amount of aldehyde
8 (21.6%) since some phosphate hydrolysis occurred with the concomitant formation of *gem*-
9 diol and cyclic hemiacetal forms of the pyridoxal molecule in 3%, according with the NMR
10 spectrum (Figure S20). Then, the pyridoxal-5'-phosphate was dissolved in DMSO-*d*₆ and
11 the results were completely different, since the aldehyde and *gem*-diol contents were 94%
12 and 6%, respectively. Once again, as in other compounds described in this work, DMSO-*d*₆
13 is not the best solvent to study the “real composition” of the samples in the solid state, but is
14 useful if the aldehyde form is desired in solution for any reason. In addition, the ¹H-NMR
15 results for the pyridoxal-5'-phosphate in D₂O-NaOH produced only the aldehyde form in
16 100% (Figure S21).
17
18
19
20
21
22
23
24
25
26
27
28
29
30
31
32
33
34
35
36
37
38

39 4. Conclusions.

40
41 By using both *ls*- and *ss*-NMR, we studied the generation and stability of the *gem*-diol forms
42 in various pyridine derivatives containing carbonyl groups. In general, *ss*-NMR was useful
43 to determine the presence of *gem*-diols in the solid state in cases where the crystals obtained
44 were not suitable for single-crystal X-ray diffraction studies or where the solvent in the *ls*-
45 NMR altered the chemical structure of the molecule under study. However, in many cases, it
46 was possible to analyze the data from both methods of structural characterization to
47 complement and enhance the knowledge in the chemistry of *gem*-diol compounds.
48
49
50
51
52
53
54
55
56

57 The limitation of analytical techniques for the characterization of the *gem*-diol/carbonyl
58 (aldehyde or ketone) content for a particular formyl or ketone compound is the balance
59
60

1
2
3 obtained in a particular solvent. For that reason, throughout the manuscript, it is mentioned
4 that for example the DMSO- d_6 solvent is not the best medium for the characterization at the
5 liquid state, being the *ss*-NMR the best technique for the screening at the solid state, taking
6 into account the inherent problem of low sensitivity. Common HPLC techniques can be
7 used, but the problem is that the sample needs to be dissolved in acid/water mixtures, being
8 easier to analyze only the NMR information from the solution state in the presence of H^+
9 species.
10

11 The hydration studies indicated that the position of the carbonyl group was essential to
12 stabilize the *gem*-diol form, allowing their isolation and characterization in the solid state.
13 The hydration process of formylpyridine compounds was favored due to the electron-
14 withdrawing character of the aromatic system, being 2- and 4-formylpyridines particularly
15 stable. Also, the oxidation to carboxylic acid in some of the compounds studied here was
16 obtained from the trifluoroacetate derivatives of formylpyridines according with the NMR
17 and X-ray results.
18

19 The structural characterization by X-ray crystallography and *ss*-NMR techniques of vitamin
20 B₆-related compounds allowed identifying a cyclic hemiacetal form for the pyridoxal
21 molecule, which was present with both TFA and HCl medium. In addition, the racemization
22 of the pyridoxal molecules demonstrated in acidic medium due to the intramolecular
23 cyclization is equally probable for both sides of the planar formyl group, rendering a
24 racemic sample that was evidenced with the X-ray results.
25

26 Indeed, the results presented here explain some structural characteristics observed in metal
27 ion complexes where the *gem*-diol, carbonyl or hemiacetal moieties are present, depending
28 on the monomer used. This would allow a smart design of new metal complexes by using
29 some of the compounds studied here and different metal ions, in a variety of experimental
30
31
32
33
34
35
36
37
38
39
40
41
42
43
44
45
46
47
48
49
50
51
52
53
54
55
56
57
58
59
60

1
2
3 conditions. This will allow expanding the chemistry in metal complexes and single-molecule
4 magnets in terms of structural diversity of the ligands.
5
6
7
8
9

10 **Acknowledgments.**

11 We thank the financial support from ANPCYT (PICT 2012-0151), Universidad de Buenos
12 Aires (UBACyT 2013-2016/043BA), CONICET (PIP 2014-2016/130) and SeCyT
13 Universidad Nacional de Córdoba. We also thank María Victoria González-Eusevi for the
14 English grammar corrections.
15
16
17
18
19
20
21
22
23

24 **Supporting Information.**

25 Structural data of **CA₃.TFA** (CCDC N°1471042), **H₄** (CCDC N°1471040), **P₅** (CCDC
26 N°1471035), **H₆.TFA** (CCDC N°1471038), **HA₇.TFA** (CCDC N°1471043) compounds were
27 deposited as CIF files at the Cambridge Crystallographic Database, and can be downloaded
28 freely from the site: <http://ccdc.cam.ac.uk>. We provide here the supplementary
29 crystallographic information for each compound and *ls*-NMR spectra for all the compounds
30 studied in the present work.
31
32
33
34
35
36
37
38
39
40
41
42

43 **References.**

- 44
45
46 (1) Tasiopoulos, A. J.; Perlepes, S. P. Diol-Type Ligands as Central “Players” in the
47 Chemistry of High-Spin Molecules and Single-Molecule Magnets. *Dalton Trans.*
48 **2008**, No. 41, 5537–5555.
49
50
51
52
53 (2) March, J. *Advanced Organic Chemistry*; Wiley: New York, 1992.
54
55
56 (3) Lázaro Martínez, J. M.; Romasanta, P. N.; Chattah, A. K.; Buldain, G. Y. NMR
57 Characterization of Hydrate and Aldehyde Forms of Imidazole-2-Carboxaldehyde and
58 Derivatives. *J. Org. Chem.* **2010**, 75 (10), 3208–3213.
59
60

- 1
2
3
4
5
6
7
8
9
10
11
12
13
14
15
16
17
18
19
20
21
22
23
24
25
26
27
28
29
30
31
32
33
34
35
36
37
38
39
40
41
42
43
44
45
46
47
48
49
50
51
52
53
54
55
56
57
58
59
60
- (4) Barszcz, B. Coordination Properties of Didentate N,O Heterocyclic Alcohols and Aldehydes towards Cu(II), Co(II), Zn(II) and Cd(II) Ions in the Solid State and Aqueous Solution. *Coord. Chem. Rev.* **2005**, *249*, 2259–2276.
 - (5) Casas, J. S.; Castiñeiras, A.; Rodríguez-Argüelles, M. C.; Sánchez, A.; Sordo, J.; Vázquez-López, A.; Vázquez-López, E. M. Diorganotin(IV) Complexes of Imidazole-2-Carbaldehyde Thiosemicarbazone (H2ImTSC). The Crystal and Molecular Structures of the “free” Ligand and of [SnMe2(ImTSC)]. *J. Chem. Soc. Dalt. Trans.* **2000**, *14*, 2267–2272.
 - (6) Perl, N. R.; Leighton, J. L. Enantioselective Imidazole-Directed Allylation of Aldimines and Ketimines. *Org. Lett.* **2007**, *9*, 3699–3701.
 - (7) Efthymiou, C. G.; Raptopoulou, C. P.; Psycharis, V.; Tasiopoulos, A. J.; Escuer, A.; Perlepes, S. P.; Papatriantafyllopoulou, C. Copper(II)/di-2-Pyridyl Ketone Chemistry: A Triangular Cluster Displaying Antisymmetric Exchange versus an 1D Coordination Polymer. *Polyhedron* **2013**, *64*, 30–37.
 - (8) Efthymiou, C. G.; Papatriantafyllopoulou, C.; Aromi, G.; Teat, S. J.; Christou, G.; Perlepes, S. P. A NiIII Cubane with a Ligand Derived from a Unique Metal Ion-Promoted, Crossed-Aldol Reaction of Acetone with Di-2-Pyridyl Ketone. *Polyhedron* **2011**, *30*, 3022–3025.
 - (9) Liu, J.-L.; Lin, W.-Q.; Chen, Y.-C.; Gómez-Coca, S.; Aravena, D.; Ruiz, E.; Leng, J.-D.; Tong, M.-L. Cu(II)-Gd(III) Cryogenic Magnetic Refrigerants and Cu8Dy9 Single-Molecule Magnet Generated by in Situ Reactions of Picolinaldehyde and Acetylpyridine: Experimental and Theoretical Study. *Chem. Eur. J.* **2013**, *19*, 17567–17577.
 - (10) Abufager, P. N.; Robles, R.; Lorente, N. FeCoCp3 Molecular Magnets as Spin Filters.

- 1
2
3
4
5
6
7
8
9
10
11
12
13
14
15
16
17
18
19
20
21
22
23
24
25
26
27
28
29
30
31
32
33
34
35
36
37
38
39
40
41
42
43
44
45
46
47
48
49
50
51
52
53
54
55
56
57
58
59
60
- J. Phys. Chem. C* **2015**, *119*, 12119–12129.
- (11) Moro, F.; Biagi, R.; Corradini, V.; Evangelisti, M.; Gambardella, A.; De Renzi, V.; del Pennino, U.; Coronado, E.; Forment-Aliaga, A.; Romero, F. M. Electronic and Magnetic Properties of Mn₁₂ Molecular Magnets on Sulfonate and Carboxylic Acid Prefunctionalized Gold Surfaces. *J. Phys. Chem. C* **2012**, *116*, 14936–14942.
- (12) Serrano, G.; Wiespointner-Baumgarthuber, S.; Tebi, S.; Klyatskaya, S.; Ruben, M.; Koch, R.; Müllegger, S. Bilayer of Terbium Double-Decker Single-Molecule Magnets. *J. Phys. Chem. C* **2016**, *120*, 13581–13586.
- (13) Woodruff, D. N.; Winpenny, R. E. P.; Layfield, R. A. Lanthanide Single-Molecule Magnets. *Chem. Rev.* **2013**, *113*, 5110–5148.
- (14) Hwan, J.; Harrowfield, J.; Young, J.; Kim, Y.; Hoon, Y.; Ohto, K.; Thuéry, P.; Seon, M.; Woo, A. Some Post-Wernerian Coordination Chemistry. *Polyhedron* **2013**, *52*, 1190–1198.
- (15) Cruz-Enriquez, A.; Baez-Castro, A.; Hopfl, H.; Parra-Hake, M.; Campos-Gaxiola, J. J. Tetrakis(μ -Acetato- $k_2O:O'$)-bis[(3-Pyridinecarboxaldehyde- kN')]-dicopper(II)(Cu—Cu). *Acta Crystallogr. Sect. E. Struct. Rep. Online* **2012**, *E68*, m1339–m1340.
- (16) Li, Y.; Liu, Z.; Deng, H. Dichloridobis(pyridine-3-Carbaldehyde- kN)zinc(II). *Acta Crystallogr. Sect. E. Struct. Rep. Online* **2007**, *E63*, m3065.
- (17) Müller, B.; Vahrenkamp, H. Zinc Complexes of Aldehydes and Ketones, Zinc Complexes of Chelating Aldehydes. *Eur. J. Inorg. Chem.* **1999**, 137–144.
- (18) Wang, W.; Spingler, B.; Alberto, R. Reactivity of 2-Pyridine-Aldehyde and 2-Acetyl-Pyridine Coordinated to [Re(CO)₃]⁺ with Alcohols and Amines: Metal Mediated Schiff Base Formation and Dimerization. *Inorganica Chim. Acta* **2003**, *355*, 386–393.

- 1
2
3
4
5
6
7
8
9
10
11
12
13
14
15
16
17
18
19
20
21
22
23
24
25
26
27
28
29
30
31
32
33
34
35
36
37
38
39
40
41
42
43
44
45
46
47
48
49
50
51
52
53
54
55
56
57
58
59
60
- (19) Cox, M.; Newman, P.; Stephens, F.; Vagg, R.; Williamst, P. Chiral Metal Complexes 40*. The Sterically Mediated Hydrolysis of a Coordinated Imine. *Inorganica Chim. Acta* **1994**, *221*, 191–196.
- (20) Bravo-García, L.; Barandika, G.; Bazán, B.; Urriaga, M. K.; Arriortua, M. I. Thermal Stability of Ionic Nets with CuII Ions Coordinated to Di-2-Pyridyl Ketone: Reversible Crystal-to-Crystal Phase Transformation. *Polyhedron* **2015**, *92*, 117–123.
- (21) Thangavel, A.; Elder, I. A.; Sotiriou-Leventis, C.; Dawes, R.; Leventis, N. Breaking Aggregation and Driving the Keto-to-Gem-Diol Equilibrium of the N,N'-Dimethyl-2,6-Diaza-9,10-Anthraquinonediium Dication to the Keto Form by Intercalation in cucurbit[7]uril. *J. Org. Chem.* **2013**, *78*, 8297–8304.
- (22) Yonekawa, M.; Furusho, Y.; Sei, Y.; Takata, T.; Endo, T. Synthesis and X-Ray Structural Analysis of an Acyclic Bifunctional Vicinal Triketone, Its Hydrate, and Its Ethanol-Adduct. *Tetrahedron* **2013**, *69*, 4076–4080.
- (23) Liu, B. Crystal Structure of Trans-diacetatobis(2,6-pyridinediylbis(3-Pyridinyl)-Methanone)-κ²N,N'-copper(II) Acetonitrile (1/2), C₄₂H₂₈CuF₆N₈O₈. *Zeitschrift für Krist. - New Cryst. Struct.* **2013**, *228*, 389–390.
- (24) Maass, G.; Ahrens, M. L.; Schuster, P.; Winkler, H. Kinetic Study of the Hydration Mechanism of Vitamin B6 and Related Compounds. *J. Am. Chem. Soc.* **1970**, *92*, 6134–6139.
- (25) Helmreich, E. J. M.; Klein, H. W. The Role of Pyridoxal Phosphate in the Catalysis of Glycogen Phosphorylases. *Angew. Chemie Int. Ed. English* **1980**, *19*, 441–455.
- (26) O'Leary, M.; Payne, J. ¹³C NMR Spectroscopy of Labeled Pyridoxal 5'-Phosphate. *J. Biol. Chem.* **1976**, *251*, 2248–2254.
- (27) Hanes, J. W.; Keresztes, I.; Begley, T. P. ¹³C NMR Snapshots of the Complex

- 1
2
3
4
5
6
7
8
9
10
11
12
13
14
15
16
17
18
19
20
21
22
23
24
25
26
27
28
29
30
31
32
33
34
35
36
37
38
39
40
41
42
43
44
45
46
47
48
49
50
51
52
53
54
55
56
57
58
59
60
- Reaction Coordinate of Pyridoxal Phosphate Synthase. *Nat. Chem. Biol.* **2008**, *4*, 425–430.
- (28) Chan-Huot, M.; Niether, C.; Sharif, S.; Tolstoy, P. M.; Toney, M. D.; Limbach, H. H. NMR Studies of the Protonation States of Pyridoxal-5'-Phosphate in Water. *J. Mol. Struct.* **2010**, *976*, 282–289.
- (29) Fung, B. M.; Khitrin, A. K.; Ermolaev, K. An Improved Broadband Decoupling Sequence for Liquid Crystals and Solids. *J. Magn. Reson.* **2000**, *101*, 97–101.
- (30) Sheldrick, G. M. Phase Annealing in SHELX-90: Direct Methods for Larger Structures. *Acta Crystallogr. Sect. A* **1990**, *46*, 467–473.
- (31) Sheldrick, G. M. A Short History of SHELX. *Acta Crystallogr. Sect. A Found. Crystallogr.* **2007**, *64*, 112–122.
- (32) Athimoolam, S.; Natarajan, S. Nicotinium Trifluoroacetate. *Acta Crystallogr. Sect. E Struct. Reports Online* **2007**, *63*, o2656–o2656.
- (33) Baias, M.; Widdifield, C. M.; Dumez, J.-N.; Thompson, H. P. G.; Cooper, T. G.; Salager, E.; Bassil, S.; Stein, R. S.; Lesage, A.; Day, G. M.; et al. Powder Crystallography of Pharmaceutical Materials by Combined Crystal Structure Prediction and Solid-State ¹H NMR Spectroscopy. *Phys. Chem. Chem. Phys.* **2013**, *15*, 8069–8080.
- (34) González Mantero, D.; Altaf, M.; Neels, A.; Stoeckli-Evans, H. Pyridin-4-Ylmethanediol: The Hydrated Form of Isonicotinaldehyde. *Acta Crystallogr. Sect. E Struct. Rep. Online* **2006**, *E62*, o5204–o5206.
- (35) Majerz, I.; Sawka-Dobrowolska, W.; Sobczyk, L. Hydrogen Bonds in 4-Dihydroxymethylpyridinium 2,6-Dichloro-4-Nitrophenolate. *J. Mol. Struct.* **1997**, *416*, 113–120.

- 1
2
3
4 (36) Bock, H.; Van, T. T. H.; Schödel, H.; Dienelt, R. Structural Changes of Di(2-Pyridyl)
5 Ketone on Single and Twofold Protonation. *European J. Org. Chem.* **1998**, 585–592.
6
7
8
9 (37) Wang, S. L.; Richardson, J. W.; Briggs, S. J.; Jacobson, R. A.; Jensen, W. P.
10 Stabilization of a Hydrated Ketone by Metal Complexation. The Crystal and
11 Molecular Structures of Bis-2,2',N,N'-Bipyridyl Ketone-Hydrate Nickel(II) Sulfate,
12 Copper(II) Chloride and Copper(II) Nitrate. *Inorganica Chim. Acta* **1986**, *111*, 67–72.
13
14
15
16 (38) Yang, G.; Tong, M. L.; Chen, X. M.; Ng, S. W. Bis(di-2-Pyridylmethanediol-
17 N,O,N')- copper(II) Diperchlorate. *Acta Crystallogr. Sect. C* **1998**, *54*, 732–734.
18
19
20
21 (39) Gansow, O. A.; Holm, R. H. Aqueous Solution Equilibria of Pyridoxamine,
22 Pyridoxal, 3-Hydroxypyridine-4-Aldehyde, and 3-Hydroxypyridine-2-Aldehyde as
23 Studied by Proton Resonance. *Tetrahedron* **1968**, *24*, 4477–4487.
24
25
26
27 (40) Sudhakar Rao, S. P.; Damodara Poojary, M.; Manohar, H. Crystal and Molecular
28 Structure of Pyridoxal. *Curr. Sci.* **1982**, *51*, 410–411.
29
30
31
32 (41) Fujiwara, T.; Izumi, Y.; Tomita, K. The Crystal and Molecular Structures of Vitamin
33 B6 Derivatives. *Acta Crystallogr. Sect. A Cryst. Phys., Diffr., Theor. Crystallogr.*
34 **1972**, *28*, S49.
35
36
37
38 (42) Fujiwara, T. The Crystal and Molecular Structure of Vitamin B6 Derivatives. I.
39 Pyridoxal Phosphate Hydrate and Pyridoxal Phosphate Methyl Hemiacetal. *Bull.*
40 *Chem. Soc. Jpn.* **1973**, *46*, 863–871.
41
42
43
44
45
46
47
48
49
50
51
52
53
54
55
56
57
58
59
60

1
2
3
4
5
6
7
8
9
10
11
12
13
14
15
16
17
18
19
20
21
22
23
24
25
26
27
28
29
30
31
32
33
34
35
36
37
38
39
40
41
42
43
44
45
46
47
48
49
50
51
52
53
54
55
56
57
58
59
60

“for Table of Contents use only”

***Gem*-diol and hemiacetal forms in formyl pyridine and vitamin-B₆-related compounds:
solid-state NMR and single-crystal X-ray diffraction studies.**

Ayelén Florencia Crespi, Daniel Vega, Ana Karina Chattah, Gustavo Alberto Monti,

Graciela Yolanda Buldain, Juan Manuel Lázaro-Martínez.

